UNIVERSITY of York

This is a repository copy of *Reaction rate for carbon burning in massive stars*.

White Rose Research Online URL for this paper:
https://eprints.whiterose.ac.uk/132196/

Version: Accepted Version

Article:
Jiang, C. L., Santiago-Gonzalez, D., Almaraz-Calderon, S. et al. (35 more authors) (2018) Reaction rate for carbon burning in massive stars. Physical Review C. 012801. ISSN 2469-9993

https://doi.org/10.1103/PhysRevC.97.012801

Reuse
Items deposited in White Rose Research Online are protected by copyright, with all rights reserved unless indicated otherwise. They may be downloaded and/or printed for private study, or other acts as permitted by national copyright laws. The publisher or other rights holders may allow further reproduction and re-use of the full text version. This is indicated by the licence information on the White Rose Research Online record for the item.

Takedown
If you consider content in White Rose Research Online to be in breach of UK law, please notify us by emailing eprints@whiterose.ac.uk including the URL of the record and the reason for the withdrawal request.

White Rose university consortium
Universities of Leeds, Sheffield & York

eprints@whiterose.ac.uk
https://eprints.whiterose.ac.uk/

The reaction rate for carbon burning in massive stars

C.L. Jiang[1], D. Santiago-Gonzalez[2,1], S. Almaraz-Calderon[1,3], K.E. Rehm[1], B.B. Back[1], K. Auranen[1], M.L. Avila[1], A.D. Ayangeakaa[1], S. Bottoni[1], M. Carpenter[1], C. Dickerson[1], B. DiGiovine[1], J.P. Greene[1], C.R. Hoffman[1], R.V.F. Janssens[1], B.P. Kay[1], S.A. Kuvin[1], T. Lauritsen[1], R.C. Pardo[1], J. Sethi[1], D. Seweryniak[1], R. Talwar[1], C. Ugalde[1], S. Zhu[1], D. Bourgin[4], S. Courtin[4], F. Haas[4], M. Heine[4], G. Fruet[4], D. Montanari[4], D. Jenkins[5], L. Morris[5], A. Lefebvre-Schuhl[6], M. Alcorta[7], X. Fang[8], X.D. Tang[9], B. Bucher[10], C.M. Deibel[2], and S.T. Marley[2]

[1] *Physics Division, Argonne National Laboratory, Argonne, IL 60439, USA*
[2] *Department of Physics and Astronomy, Louisiana State University, Baton Rouge, LA70803, USA*
[3] *Department of Physics, Florida State University, Tallahassee, FL 32306, USA*
[4] *IPHC and CNRS, Universite de Strasbourg, F-67037 Strasbourg, France*
[5] *Department of Physics,University of York, Heslington, York YO10 5DD, UK*
[6] *IN2P3-CNRS and University of Paris Sud, F-91405 Orsay-campus, France*
[7] *TRIUMF, Vancouver, BC V6T 2A3, Canada*
[8] *University of Notre Dame, Notre Dame, IN 46556, USA*
[9] *Institute of Modern Physics, Lanzhou, China and*
[10] *Lawrence Livermore National Laboratory, Livermore, CA 94551, USA*

(Dated: December 22, 2016)

Carbon burning is a critical phase for the nucleosynthesis in massive stars. The conditions for igniting this burning stage, and the subsequent isotope composition of the resulting ashes, depend strongly on the reaction rate for ^{12}C + ^{12}C fusion at very low energies. Measurements of the cross section for this reaction are strongly influenced by various backgrounds encountered in experiments at low energies. In this paper we report on new a measurement of ^{12}C+^{12}C fusion cross sections where these background problems have been eliminated. It is found that the astrophysical S factor exhibits a maximum at around E = 3.5-4.0 MeV which leads to a reduction of the previously predicted astrophysical reaction rate.

PACS numbers: 25.70.Jj, 26.30.-k, 24.10.Eq, 24.30.Gd

When a massive star has exhausted its supply of hydrogen and helium, it contracts under the gravitational pressure leading to an increase in the temperature. At these elevated temperatures the ashes of helium burning (i.e. ^{12}C) can ignite and initiate the so-called carbon burning phase [1, 2]. The ^{12}C + ^{12}C fusion reaction is an important route for the production of elements with A≥20, and it also influences the later nucleosynthesis processes, such as the slow and rapid neutron-capture processes [3].

In explosive scenarios such as in type Ia supernovae carbon burning occurs at higher temperatures. While experimental data relevant for this energy regime can be found in the literature [4–11] the associated Gamow energies are still quite low, resulting in small cross sections which are in many cases influenced by background reactions. Furthermore, as discussed in Ref. [9] there are 20-100 keV energy shifts between the excitation functions measured by different groups resulting in large variationss of the ^{12}C + ^{12}C fusion cross sections.

For quiescent carbon burning in massive stars the Gamow window is so low that no experimental data exist in this energy regime. Phenomenonological extrapolations or model calculations are therefore needed in order to obtain the astrophysical reaction rate of the ^{12}C + ^{12}C reaction. For this extrapolation several predictions can be found in the literature [12–15].

A summary of the experimental data that can be found in the literature is given in Fig. 1 in a plot of the S factor ($S(E) = \sigma E e^{2\pi\eta}$) [4–11], where E is the center-of-mass energy, σ is the fusion cross section and η is the Sommerfeld parameter. The Gamow energy associated with quiescent carbon burning in massive stars is less than 2 MeV, which is outside of the energy region shown in Fig. 1 [16].

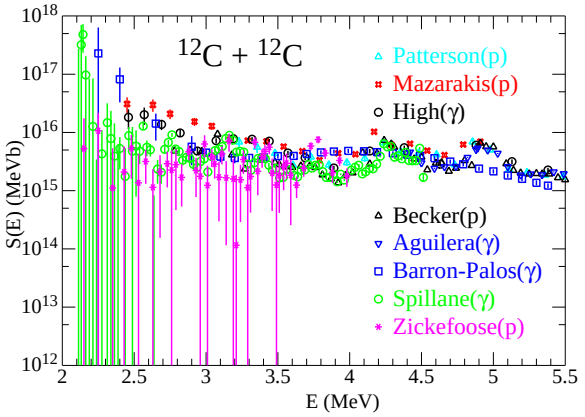

FIG. 1: (Color online) $S(E)$ factors from previous measurements of the ^{12}C + ^{12}C fusion reaction. Charged-particle detections are used in the measurements from Patterson, Mazarakis, Becker and Zickefoose, while γ-ray detections are employed in the measurements of High, Barron-Palos, Auguilera and Spillane.

As can be seen in Fig. 1 the experimental cross sections in the energy region of E=3-4.5 MeV differ by up to one

order of magnitude. The two most recent experiments, performed by Spillane *et al.*, [10] and by Zickefoose *et al.*, [11] shown in Fig. 1 by the magenta and green symbols, respectively, used two different detection techniques. In Ref. [10] the γ-rays of the evaporation residues were detected, while Ref. [11] measured the charged particles emitted by the evaporation residues. The large uncertainties in these two experiments at the lowest energies are caused by both, the background encountered by the γ- and charged-particle-detection techniques and by the thick-target method which requires to subtract two spectra taken at slightly different energies. While Ref. [10] claimed to have observed a resonance at about 2.14 MeV, the later measurement [11] obtained cross sections in the same energy region which were smaller by about two orders of magnitude.

In order to obtain accurate cross sections of ^{12}C + ^{12}C fusion at low energies, a reduction of the background is essential. For that purpose we have developed a particle-γ coincidence technique that eliminates these backgrounds and provides reliable fusion cross sections for the ^{12}C + ^{12}C system [17]. In this article we present results from measurements using this technique and discuss their impact on the astrophysical reaction rates of carbon burning and on the theory of fusion reactions.

The experiment was performed at the ATLAS accelerator at Argonne National Laboratory using Gammasphere (GS) which is an array of about 100 Compton-suppressed Ge-detectors [18] to detect the γ rays from the ^{20}Ne and ^{23}Na evaporation residues. The coincident charged particles emitted from the evaporation residues were identified in a compact array of three annular double-sided silicon surface barrier detectors (DSSD1, DSSD2 and DSSD3) located inside GS. A schematic plot of the experimental setup is shown in Fig. 2. Each Si detector had a thickness of 500 μm and was subdivided into 16 rings and 16 wedges covering the angular range of 147-170°, 123-143° and 17-32°, respectively. The total solid angle coverage was about 25% of 4π. In order to reduce the count rate from elastically scattered ^{12}C ions and from other background reactions (*e.g.* ^{12}C + H $\rightarrow$ p and ^{12}C + D $\rightarrow$ p or d) aluminum absorber foils were placed in front of each DSSD. A Faraday cup and two monitor detectors were used for beam normalization. In addition, an image sensor sensitive to infrared light was installed to monitor the beam spot size and location during the runs. Contrary to the measurements in Ref. [10, 11] this is a thin-target experiment which does not require to subtract spectra taken at different energies.

Isotopically enriched ($\geq$ 99.9%) ^{12}C targets of about 40-50 μg/cm^2 were used. Since in experiments using γ-ray detection techniques transitions populating the ground states in ^{23}Na and ^{20}Ne (*e.g.* ^{12}C + ^{12}C $\rightarrow$^{23}Na$_{gs}$ + p$_0$) cannot be measured corrections to the total fusion cross section have to be applied using previously measured yields from charged-particle experiments (see *e.g.* Ref. [8]). This correction was about 13% at the lowest energy.

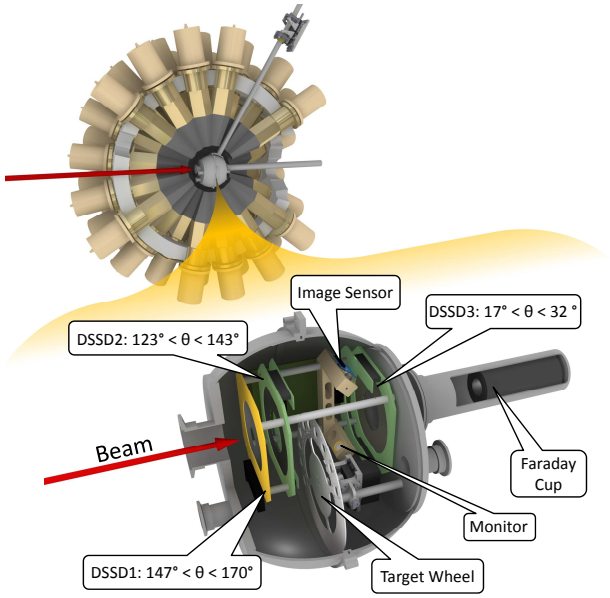

FIG. 2: (Color online) A schematic plot of the experimental setup showing the spherical-target chamber mounted in the middle of the Gammasphere array.

Measurements were performed at ten beam energies between E_{lab}=10-5.5 MeV. Maximum beam currents were about 600 pnA. The beam energy for each measurement was determined using the split-pole magnetic spectrograph, which was calibrated with standard $\alpha-$sources. A detailed description of the experiment and the resulting reduction in background using the particle-γ coincidence technique can be found in Ref. [17].

Particle-γ coincidence events from the ^{12}C(^{12}C,p)^{23}Na fusion reaction populating the first excited state in ^{23}Na at E$_x$=0.440 MeV measured in DSSD1 at the second lowest energy, E_{cm}=2.84 MeV are shown in Figs. 3a and 3b. The 440 keV γ-rays emitted from the fusion evaporation residues ^{23}Na$_{1st}$ in coincidence with protons, p_1 of energies of $\sim$ 2.2 MeV are located in the rectangular region in Fig. 3a. In a plot of scatterimg angle vs. particle energy, these events follow the kinematics expected for the ^{12}C(^{12}C,p$_1$)^{23}Na$_{1st}$ reaction as shown by the dashed line (and the band) in Fig. 3b.

Similar results are obtained for the ^{12}C(^{12}C,α)^{20}Ne reaction by gating on the 1.635 MeV, $2^+ \rightarrow 0^+$ transition in ^{20}Ne, as shown in Figs. (3c) and (3d) for the third lowest energy, E=2.96 MeV, in DSSD2. As can be seen in Fig. 3 there are two groups of coincident particles α_1 and p$_2$ because a γ-ray of 1.635 MeV can originate from the decay of the 2^+_1 state in ^{20}Ne which is in coincidence with an α particle but also from the decay of the $7/2^+_1$ state to the $5/2^+_1$ state in ^{23}Na (E$_\gamma$=1.64 MeV) which is in coincidence with a proton showing the high resolving power of the particle-γ-coicidence technique.

The total coincidence efficiency determined from the angle coverage of the DSSD's and the efficiency of γ-ray detection was found to be around 9-7 % for E_γ=440

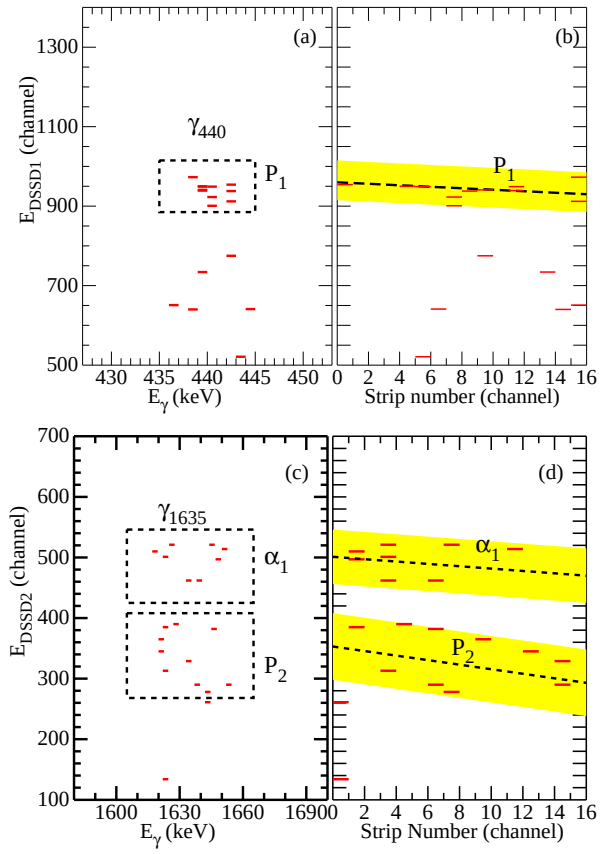

FIG. 3: (Color online) (a) Particle-γ coincidence events detected by DSSD1 located at backward angles at the second lowest energy studied in this experiment, E=2.84 MeV. (b) Energy-angle correlation of the coincident particle-γ events shown in the rectangular region in Fig. 2b. The dashed line represents the kinematic expected for the ^{12}C(^{12}C,p)^{23}Na reaction populating the 0.440 MeV state in ^{23}Na. (c) and (d) are plots similar to (a) and (b) but measured for the third lowest energy, E_{cm}=2.96 MeV. The dashed lines represents the kinematic expected for the ^{12}C(^{12}C,α)^{20}Ne and ^{12}C(^{12}C,p)^{23}Na reactions. See text for details.

and 1635 keV, respectively. The relative yields of the residues ^{23}Na and ^{20}Ne was around 0.9-1.6 in the energy region from E= 4.93-2.68 MeV. Results of the measured total fusion cross sections are listed in Table I. The cross section at 4.93 MeV, 4.8 $\pm$ 0.9 mb is in good agreement with the result of Ref. [8].

The cross sections measured in this experiment converted into astrophysical S factors are shown by the black open circles in Fig. 4. They are in good agreement with the recent measurements using γ-detection [10], but have smaller uncertainties, since it was a background free measurement and results were not obtained by the thick-target technique. It should be noted that the cross sections at the lowest energy point of the present measurement coincides with the result of Spillane et al.[10].

Four results of model calculations and extrapolations into the low-energy region are included in Fig. 4. The

TABLE I: Present measured results for fusion cross sections of ^{12}C + ^{12}C.

E	σ	$\Delta\sigma$	S factor	ΔS
MeV	mb	mb	10^{15}MeVb	10^{15}MeVb
4.93	4.8	0.9	2.8	0.5
4.80	2.0	0.4	1.9	0.4
4.73	0.88	0.17	1.1	0.2
4.53	0.92	0.18	2.6	0.5
4.22	0.50	0.10	6.0	1.2
3.93	0.070	0.014	3.6	0.7
3.43	0.0041	8.1x10^{-4}	4.0	0.8
2.96	9.5E-5	1.9x10^{-5}	3.0	0.6
2.84	4.0E-5	2.0x10^{-5}	3.5	1.8
2.68	6.2E-6	3.1x10^{-6}	2.3	1.2

earliest extrapolation from Fowler and Caughlan is shown by the light blue curve [12]. Esbensen calculated the cross sections in this energy region with the so-called sudden model (magenta dashed curve) [14]. It was pointed out in Ref. [15] that for the fusion reaction of ^{12}C + ^{12}C $\rightarrow$ ^{24}Mg, the level density in the compound nucleus ^{24}Mg is low and the level widths are small. Therefore the conditions for using the incoming wave boundary condition in the CC calculations are not fulfilled. A calculation where this correction was included [15] is presented in Fig. 4 by the black curve.

The S factors from these three extrapolations increase with decreasing energy, contrary to the extrapolation which is based on the hindrance recipe described in Ref. [13] (shown by the red curve in Fig. 1). This extrapolation will be discussed in more detailed later.

In the region of the lowest energies measured in this experiment the data do not agree with an increase of $S(E)$ predicted by Fowler [12], Esbensen [14] and Jiang [15]. Instead we note that the S factor appears to decline towards the lower energy region and exhibits a weak maximum around 3.5-4 MeV, a behavior similar to the hindrance phenomenon found ten years ago in reactions between medium mass nuclei [19, 20], where it was observed that at low energies the fusion cross sections fall off faster than expected by coupled-channels (CC) calculations using standard Woods-Saxon potentials. This steep fall-off produces a maximum in the $S(E)$ factor at low energies. Since for these medium-mass systems, the fusion Q values are usually negative there has to be an $S(E)$-factor maximum because $\sigma = 0$ at energies $E \leq -Q$ [21]. For these systems the maximum of the S factor occurs typically at excitation emergies of the compound system of 20-40 MeV.

Two approaches have been proposed to describe the occurence of fusion hindrance at low energies. In the 'sudden model' Mişicu and Esbensen [22] introduce a repulsive core in the interaction potential to describe the saturation property of nuclear matter. Ichikawa *et al.* [23] developed an adiabatic model to explain the fusion hindrance by introducing a damping factor for the coupling strength in the region where the two colliding par-

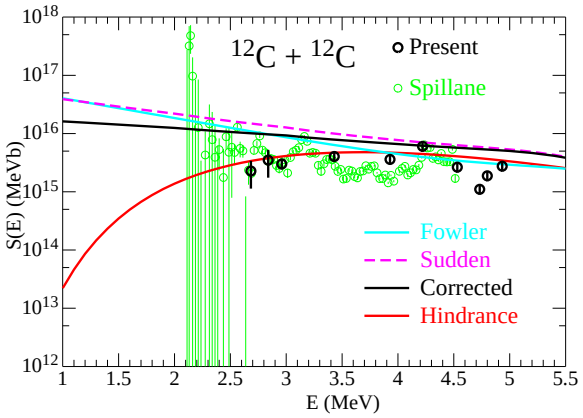

FIG. 4: (Color online) Black open points: $S(E)$ factors from the present measurements of the ^{12}C + ^{12}C fusion reaction. Green open circles: results from the recent measurement of the same system [10]. The light blue, magenta-dashed, black and red lines are calculations explained in the text.

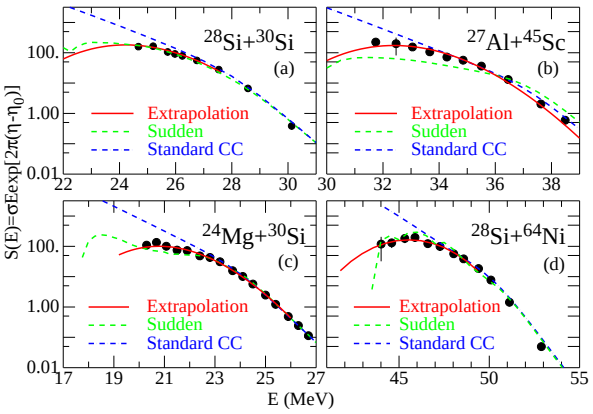

FIG. 5: (Color online) $S(E)$ factors for systems ^{28}Si + ^{30}Si (a), ^{27}Al + ^{45}Sc (b), ^{24}Mg + ^{30}Si (c), and ^{28}Si + ^{64}Ni (d). The fusion Q-values are 14.3, 9.63, 17.89 and -1.87 MeV, respectively.

ticles come into contact.

More recently fusion hindrance has also been studied for systems with positive Q values. Contrary to fusion reactions with negative Q values these systems do not require the existance of an $S(E)$-factor maximum, since even at $E = 0$ the fusion cross sections can have a finite value. Some examples are presented in Fig. 5 [24–27]. for the systems ^{28}Si + ^{30}Si, ^{27}Al + ^{45}Sc and ^{24}Mg + ^{30}Si [24] with positive fusion Q values (Q=14.3, 9.63 and 17.89 MeV, respectively), while for ^{28}Si + ^{64}Ni, shown in Fig. 5d, the Q value is negative, -1.78 MeV.

Three kinds of extrapolations are included in Fig. 5. The blue dashed curves are CC calculations with a standard Woods-Saxon potential, which always overpredict the experimental data at low energies. The green-dashed curves are CC calculations with a repulsive core included in the potential (sudden model) while the red curves are from the empirical extrapolations ([13]) using the same recipe as used for the red line in Fig. 4. For these medium-mass systems, the calculations based on the sudden model reproduce the experimental data quite well as can be seen by the green-dashed lines.

This, however, is not the case for the ^{12}C + ^{12}C system which shows a broad, but noticable maximum in the S factor. The shape of the excitation function shown by the black points in Fig. 4 is similar to the ones presented in Fig. 5 indicating the existence of fusion hindrance in this system. However, sudden model calculations including a repulsive core [14], (see magenta dashed line in Fig. 4) show an increase of the S factor towards lower energies in disagreement with the experimental data. The only extrapolation able to describe the excitation functions presented in Fig. 4 is the red curve which is based on the extrapolation recipe developed in Ref. [13] by using three fit parameters.

Using the system dependence of the these fit parameters as described in Ref. [13, 24–26] one gets the red lines in Figs. 4 and 5a-5c, which are in very good agreement with the experimental data, including the ^{12}C + ^{12}C system where all previous extrapolations show an increase towards lower energies that is a variance with the new data.

The consequences of a reduced astrophysical reaction rate for the ^{12}C + ^{12}C fusion reaction have been discussed in Ref. [28]. The smaller cross sections and the resulting reduced reaction rates shift the ignition of carbon burning in massive stars to higher temperatures and densities and also enhances the abundance of long-lived radio-isotopes such as ^{26}Al and ^{60}Fe. A higher ^{26}Al yield would be in agreement with observations [29].

The isotope ^{60}Fe ($T_{1/2}$=2.61 My) is of particular interest since its detection in deep-sea sediments [30–32] and on the lunar surface [33] has been associated with recent (∼2.8 My) and close (∼10 pc) supernova explosions in our galaxy. Calculations with a reduced ^{12}C + ^{12}C reaction rate for a $20M_{\odot}$ star predict an increase in ^{60}Fe by about a factor of two [28] which would influence the time and distance of these supernova explosions. It should be noted, however, that different nucleosynthesis models show similar variations in the ^{60}Fe production [34].

In summary, fusion cross sections of ^{12}C + ^{12}C have been measured down to about 6 nb by using a particle-γ coincidence technique, which eliminates the backgrounds that plagued earlier experiments. The cross sections when converted into S factors show a broad maximum indicating the effect of fusion hindrance even for such a light system. Fusion hindrance necessitates a different extrapolation method towards lower energies which leads to smaller astrophysical reaction rates for various astrophysical scenarios and give a challenge to fusion reaction theory.

This work was supported by the US Department of Energy, Office of Nuclear Physics, under Contract No. DE-AC02-06CH11357 and uses resources from ANL's ATLAS facility, which is a DOE Office of Science User fa-

cility. D.S.G. and C.M.D. acknowledge the support by the same Office of Nuclear Physics, under grant No. DE-FG02-96ER40978.

[1] C.E. Rolf and W.S. Rodney, Cauldrons in the Cosmos (The University of Chicago Press, 1988).
[2] S.G. Ryan, A.J. Norton, Stellar Evolution and Nucleosynthesis (University of Chicago Press, 2010).
[3] M.E. Bennett *et al.,* Nuclear Physics in Astrophysics IV, Journal of Physics: Conference Series **202**, 012013 (2010).
[4] L.J. Patterson, H. Winkler, and C.S. Zaidins, Astrophys. J. **157**, 367 (1969).
[5] M. Mazarakis *et al.,* Phys. Rev. **C 7**, 1280 (1973).
[6] M.D. High and B. Cujec, Nucl. Phys. **A 282**, 181 (1977).
[7] H.W. Becker, K.U. Kettner, C. Rolfs, and H.P. Trautvetter, Z. Phys. **A 303**, 305 (1981).
[8] L. Barron-Palos *et al.,* Nucl. Phys. **A 779**, 318 (2006).
[9] E.F. Aguilera, *et al.,* Phys. Rev. **C 73**, 064601 (2006).
[10] T. Spillane *et al.,* Phys. Rev. Lett. **98** 122501 (2007).
[11] J. Zickefoose, Thesis, U. Conn., (2011) or www.lsw.uni-heidelberg.de/nic2010/talks/Strieder.pdf.
[12] W. Fowler, G. Caughlan and B. Zimmerman, Annu. Rev. Astrophys. **13**, 69 (1975); G.R. Caughlan and W.A. Fowler, At. Data Nucl. Data Tables, **40**, 283 (1988).
[13] C.L. Jiang, K.E. Rehm, B.B. Back and R.V.F. Janssens, Phys. Rev. **C 75**, 015803 (2007), and references therein.
[14] H. Esbensen, X.D. Tang, and C.L. Jiang, Phys. Rev. **C 84**, 064613 (2011).
[15] C.L. Jiang *et al.,* Phys. Rev. Lett. **110,** 072701 (2013).
[16] White paper on Nuclear Astrophysics and Low Energy Nuclear Physics, Journary 31, 2015
[17] C.L. Jiang *et al.,* Nucl. Instru. Meth. **A 682**, 12 (2012).
[18] I.Y. Lee, Nucl. Phys. **A 520**, 641C (1990).
[19] C.L. Jiang *et al.,* Phys. Rev. Lett. **89,** 052701 (2002).
[20] B.B. Back, H. Esbensen, C.L. Jiang and K.E. Rehm, Rev. Mod. Phys. **86**, 317 (2014).
[21] C.L. Jiang, H. Esbensen, B.B. Back, R.V.F. Janssens, Phys. Rev. **C 69,** 014604 (2004).
[22] S. Mişicu and H. Esbensen, Phys. Rev. Lett. **96**, 112701 (2006); Phys. Rev. C **75**, 034606 (2007).
[23] Ichikawa T. Ichikawa, K. Hagino and A. Iwamoto, Phys. Rev. C **75**, 057603 (2007); Phys. Rev. Lett. **103**, 202701 (2009); T. Ichikawa, K. Matsuyangi, Phys. Rev. C **88**, 011602(R) (2013).
[24] C.L. Jiang *et al.,* Phys. Rev. **C 78,** 017601 (2008).
[25] C.L. Jiang *et al.,* Phys. Rev. **C 81,** 012611 (2010).
[26] C.L. Jiang *et al.,* Phys. Rev. Lett. **113,** 0227011 (2013).
[27] C.L. Jiang *et al.,* Phys. Lett. **B 640**, 18 (2006).
[28] L.R. Gasques *et al.,* Phys. Rev.. **C 76**, 035802 (2007).
[29] M. Limongi and A. Chieffi, Astrophys. J. **647**, 483 (2006).
[30] K. Knie *et al.,* Phys. Rev. Lett. **83**, 18 (1999).
[31] K. Knie *et al.,* Phys. Rev. Lett. **93**, 171103 (2004).
[32] A. Wallner *et al.,* Nature **532**, 69 (2016).
[33] L. Fimiani *et al.,* Phys. Rev. Lett. **116**, 151104 (2016).
[34] D. Breitschwerdt *et al.,* Nature **532**, 73 (2016).